A Photoplethysmography Wearable with Long-term Heart Rate Variability Detection Algorithm

Bill Chieng, Fivos Kavassalis, Franco Baudino, and Ulkuhan Guler
Department of Electrical and Computer Engineering,
Worcester Polytechnic Institute, Worcester, MA, 01609 USA

***Abstract*—This paper presents a wearable device that extracts and utilizes a photoplethysmogram waveform to measure and estimate various vital signs via a mobile application's custom-designed algorithms. These vital signs include peripheral oxygen saturation, heart rate, respiratory rate, and short/long term heart rate variability. The device wirelessly transmits accumulated data to a mobile phone and a personal computer over Bluetooth Low Energy. Moreover, this paper explores the proposed device as an emerging technology with the Coronavirus Disease 19 (COVID-19) pandemic's contemporary concerns. The peripheral oxygen saturation measurements would give an early indicator of degrading respiratory health before the apparent manifestation of symptoms. The convenient use of this device in a mobile setting is especially relevant to current isolation precautions in place and its critical role in improving at-risk patients' care.**

I. Introduction

Oxygen is an essential molecule to facilitate cellular respiration, which is crucial for necessary life processes [1]. A patient can develop hypoxemia with a lower oxygen intake where the patients' blood oxygen saturation level is below normal. Hypoxemia can then lead to hypoxia, where the tissues of the body lack sufficient oxygen. This lack of oxygen can lead to tissue necrosis and irreversible cell death as well as other health complications [2]–[4]. For these reasons, an accurate measurement of blood oxygen level is crucial for physicians to assess a patient's health.

Medical professionals use photoplethysmogram (PPG) technology for patients because it is a non-invasiveness and quick setup. By employing other signal processing tools, the PPG waveform can also produce the patient's heart rate, respiratory rate, heart rate variability, and arterial stiffness. Heart and respiratory rates are basic vital signs that all health providers look for in patients. It is less commonly known that heart rate variability measures each patient's heartbeats' time variability and is controlled in part by a patient's automatic nervous system. Other work has also shown that PPG can also measure arterial stiffness by analyzing the peaks and time delays of the PPG waveform [5].

Devices like the proposed PPG platform that can monitor and report critical vital signals open a new medicine era. Wireless connectivity would grant patients more comfort and freedom while the health provider monitors them continuously. This paper proposes a prototype wireless PPG acquisition system that, aside from SpO_2, also reports respiratory rate, heart rate, and heart rate variability to an application on a mobile phone. The data collected is then stored in an online real-time database. Section II explains the details of the system architecture. Section III presents the various algorithms developed. Section IV display the experimental results and the related discussion, and Section V concludes.

II. System Overview

The pulse oximeter system consists of a power management block, the analog front-end (AFE), light-emitting diode (LED) driving circuit, the microcontroller (ESP32 Pico) with a build-in Blue Tooth Low Energy (BLE) communication module, and a companion app. Fig. 1 illustrates the top-level diagram of the system. The subblock are explained in the following subsections.

A. Analog Hardware Components

The power management system consists of a low-drop-out voltage regulator that takes an external battery supply and regulates it to the necessary 3.3 V voltage supply for the rest of our system.

The LED driving circuit follows an H-bridge configuration, as the ELM-4002 LED package contains both red and infrared (IR) LEDs that are anti-parallel with each other.

On the top half of the H-bridge, the PMOS transistors act as switches controlling which direction current will flow through the ELM-4002 package. The NPN transistors at the bottom of the H-bridge are controlled using DAC signals that set the amount of current allowed to flow through the LEDs to controls their respective light intensities.

Fig. 1. also depicts the circuit schematic of the analog front-end. The photodiode (PD) converts light energy reflected by the tissue and generates a proportional current. The transimpedance amplifier then amplifies this current with a feedback resistor of 200 kΩ. A 10 pF feedback capacitance C_f is placed parallel to the resistor to ensure the amplifier's stability.

The PPG signal enters a low pass filter with a -3dB frequency of 15 Hz to attenuate unwanted high-frequency noise. This subsequent signal represents the DC component, which is then fed into one of the ESP32's analog to digital converter (ADC) inputs and continues down the AFE signal circuit. The filtered DC signal goes through a voltage buffer amplifier onto an AC coupled non-inverting amplifier. In this AC coupled amplifier, the signal undergoes a high pass filter designed with 0.7 Hz corner frequency to block the DC portion of the signal allowing the AC signal of the PPG to be amplified by 100 V/V.

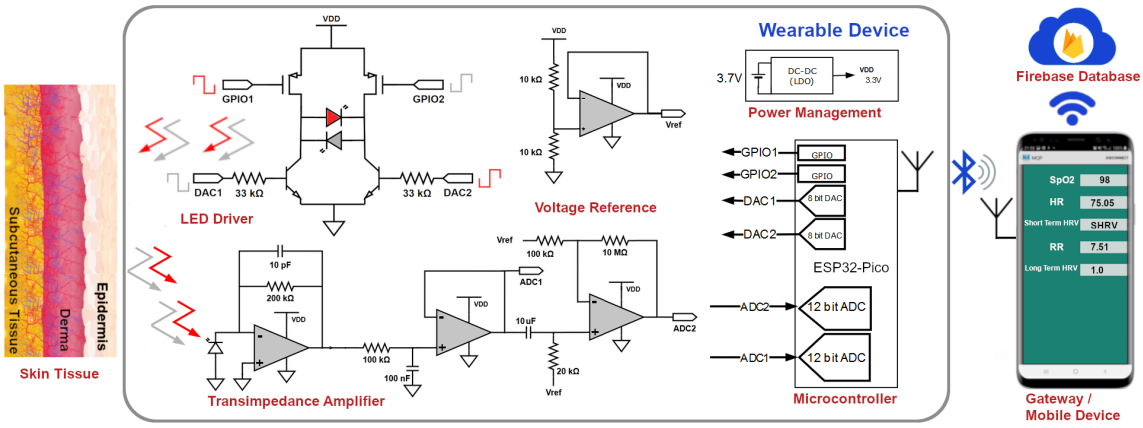

Fig. 1. Top-level block diagram

B. Microcontroller and ADC

The microcontroller, ESP32 Pico, handles the data collection from the AFE and provides the required signals to operate the LED drivers. As well as transmit the raw data to a mobile platform. The ESP32 is capable of working in different power modes. The primary operation modes utilized is the active mode and modem sleep mode. The former has all the features of the ESP32 on, particularly the BLE module for transmitting data. In contrast, modem sleep mode is less power-intensive and primarily used to send control signals through various general-purpose pins and its two integrated DACs while also reads signals from its two integrated 12-bit ADCs.

The ESP32's 8-bit digital to analog converter (DAC) can provide 256 levels between 0 V to 3.3 V. The ESP32's control signals switch on the red and IR LEDs alternately at 10 kHz frequency. The incident light from the IR and red LEDs shines into the tissue bed, and the PD receives the reflected light.

C. Mobile Application

The proposed companion application can monitor and estimate various vital signs via custom-designed algorithms. These vital signs include peripheral oxygen saturation, heart rate, respiratory rate, and both short-term and long-term heart rate variability. The mobile application was developed using the Android Studio and Google's Firebase platform to push and pull the data.

III. Algorithms

This section discusses the various algorithms implemented within the Android mobile application to extract vital sign parameters from the collected PPG signals.

A. Peripheral Oxygen Saturation (SpO_2)

The focal purpose of pulse oximetry is extracting the peripheral oxygen saturation values. The algorithm implemented for this extraction is illustrated in Algorithm 1.

To obtain the subject's blood oxygen level, 2 minutes and 10 seconds of data (sampling frequency was set to 250 Hz), with the number of samples distributed equally between the red and IR LED, were transmitted from our device over BLE to our Android application periodically. Two elements from the BLE data were the DC components for the red and IR PPG waveforms. The rest of the transmitted data were related to calculate the AC components for PPG waveforms.

Algorithm 1 SpO_2 Algorithm

```
procedure SpO2(PPG ARRAY ALL[])
    Initialize variables
    Copy RED and IR PPG values to separate arrays
    Perform FFT to the IR and RED PPG array
    for i = 0 → 8192 do
        abs_red_ppg_arr[i] ← red_ppg_arr[i].abs()/array_length
        abs_ir_ppg_arr[i] ← ir_ppg_arr[i].abs()/array_length
        freq_values[i] ← (sampling_frequency*i)/array_length
    for i = 1 → 8191 do
        abs_red_ppg_arr[i] ← 2*abs_red_ppg_arr[i]
        abs_ir_ppg_arr[i] ← 2*abs_ir_ppg_arr[i]
    red_DC_val and ir_DC_val were received from device over BLE
    for i = 1 → 8191 do
        freq ← freq_values[i]
        if freq ≥ 0.5 && freq ≤ 5 then
            if local_max_red ¡ abs_red_ppg_arr[i] then
                local_max_red ← abs_red_ppg_arr[i]
            if local_max_ir < abs_ir_ppg_arr[i] then
                local_max_ir ← abs_ir_ppg_arr[i]
    red_AC_val ← local_max_red
    ir_AC_val ← local_max_ir
    Calculate R from Equation 1
    SpO2_percentage = 115 - R × 25
    return SpO2_percentage
```

A digital sixth-order Butterworth Low Pass filter with a cutoff frequency of 5 Hz was applied to the AC component of the PPG waveform data to reduce the noise of these two signals. These signals were read by the microcontroller's ADC and concurrently accentuated the desired frequencies used to extract the AC components for SpO_2. Subsequently, spectral analysis was performed using the Fast Fourier Transform (FFT) on both waveforms. After computing the one-sided spectrum for the red and IR PPG waveforms, their AC components were determined by locating the peak in the full span of the cardiac frequency range (0.5 - 5 Hz). The resolution of the transforms was equal to approximately 0.0153 Hz. From these extracted values, the algorithm computed the SpO_2 ratio "R" by dividing the normalized red and IR AC components, which was given by the following equation:

Algorithm 2 Heart Rate Algorithm

```
1: procedure HEART RATE(PPG ARRAY ALL[])
2:     Initialize variables
3:     Copy RED PPG values to an array
4:     Perform FFT to the RED PPG array
5:     for i = 0 → 8192 do
6:         abs_red_ppg_arr[i] ← red_ppg_arr[i].abs()/array_length
7:         freq_values[i] ← (sampling_frequency*i)/array_length
8:     for i = 1 → 8191 do
9:         abs_red_ppg_arr[i] ← 2*abs_red_ppg_arr[i]
10:    for i = 1 → 8191 do
11:        freq ← freq_values[i]
12:        if freq ≥ 1 && freq ≤ 4 then
13:            if local_max_red < abs_red_ppg_arr[i] then
14:                red_local_max_index ← i
15:    return (heart_rate←freq_values[red_local_max_index]*60)
```

$$R = \frac{\left(\frac{redACval}{redDCval}\right)}{\left(\frac{irACval}{irDCval}\right)} \tag{1}$$

Finally, the algorithm was able to calculate the oxygen saturation (SpO_2) percentage by applying the empirical formula given on line 23 in Algorithm 1 with the ratio "R." The constants displayed in the equation above were validated by concurrently testing our device against a commercial pulse oximeter [6].

B. Heart Rate

The process of extracting the heart rate mirrors the SpO_2 extraction closely. However, obtaining the heart rate can be done with one PPG waveform instead of two. Additionally, the frequencies of interest for healthy patients range from 1 to 1.7 Hz (60 to 100 bpm); however, the algorithm searched up to 4 Hz to capture a greater span of the cardiac frequency range and potentially spot problematic heart rate levels. Upon locating the harmonic peak in this range of frequencies, the resultant is multiplied by 60 to get the final result as beats per minute. In other words, the heart rate was measured accordingly in line 15 of the Algorithm2 [7] [8].

C. Respiratory Rate

The respiratory rate extraction from a given PPG signal follows the same protocols as the heart rate algorithm. However, the frequencies of interest are shifted towards the DC component. The algorithm focused on the band between 0.05 and 0.7 Hz, which corresponds to 3 and 42 breaths per minute. The predominant respiratory frequency is also multiplied by 60 to get breaths per minute, as displayed in line 15 of the Algorithm 3 (denoted as respiratory_rate).

D. Heart Rate Variability

Currently, there is no universal agreement for the best HRV index. However, there are two main types of algorithms: short-term and long-term heart rate variability evaluation. We developed algorithms for both types. For the former, six HRV indices were calculated in the time domain. For the latter, spectral analysis was performed. The critical short-term heart rate variability characteristics are outlined in Table I.

1) Short-Term: The complete algorithm that was used to calculate the six short-term HRV indices as listed in Table I. The baseline used to compare the results is indicated in Table IV.

Algorithm 3 Respiratory Rate Algorithm

```
1: procedure RESPIRATORY RATE(PPG ARRAY ALL[])
2:     Initialize variables
3:     Copy RED PPG values to an array
4:     Perform FFT to the RED PPG array
5:     for i = 0 → 8192 do
6:         abs_red_ppg_arr[i] ← red_ppg_arr[i].abs()/array_length
7:         freq_values[i] ← (sampling_frequency*i)/array_length
8:     for i = 1 → 8191 do
9:         abs_red_ppg_arr[i] ← 2*abs_red_ppg_arr[i]
10:    for i = 1 → 8191 do
11:        freq ← freq_values[i]
12:        if freq ≥ 0.05 && freq ≤ 0.7 then
13:            if local_max_red < abs_red_ppg_arr[i] then
14:                red_local_max_index ← i
15:    return (respiratory_rate←freq_values[red_local_max_index]*60)
```

TABLE I: Short-Term HRV Indices

HRV Indices	Calculation Methods	Physiological Indications
SDNN	Standard deviation of NN intervals	Measure of the overall variability in HR
COV	Coefficient of variance (normalized SDNN)	Changes in overall variability independent of changes in mean NNinterval
SDSD	Standard deviation of successive NN differences	Reflection of parasympathetic influence on the heart.
RMSSD	Root-mean-square of successive NN differences	Reflection of parasympathetic influence on the heart.
NN50	Number of successive NN differences $>$ 50 ms	Index of vagal tone
pNN50	Proportion of successive NN differences greater $>$ 50ms (NN50 / Number of NN differences)	Normalized version of NN50, independent of HR

2) Long-Term: First, we needed to collect around 24 hours worth of PPG waveform data. Once all the PPG data is received, the algorithm performs spectral analysis to the data by initially applying an FFT and then calculating the power spectral density (PSD). Low-frequency signal fluctuations reflect activity in the autonomic nervous system [7]. More precisely, sympathetic activity is defined by the power in the 0.01 to 0.15 Hz range, while the power defined in parasympathetic activity is in the 0.15 to 0.5 Hz range. Therefore, the algorithm located the most significant amplitude in both of these regions, respectively. The peak in the 0.01 - 0.15 Hz region is called the "LF component," while the peak in the 0.15 - 0.5 Hz region is called the "HF component." Then, the power ratio (LF/HF) was calculated, which directly displays changes in sympathetic and parasympathetic activity. This ratio between sympathetic and parasympathetic activity represents long term HRV evaluation.

IV. Results and Discussion

The SpO_2 and heart rate values generated by the algorithm are displayed for the patient through the mobile app and the Firebase database. The results from experimental testing are shown in the following Table II.

The chart utilize four sets of measurements to evaluate the device's performance. A key consideration regarding these

TABLE II: Numerical results for SpO_2 and Heart Rate

	Masimo Rad-8		This work		Percent Error	
	(%)	(bpm)	(%)	(bpm)	(%)	(%)
Test	SpO2	HR	SpO2	HR	SpO2	HR
1	97.96	68.38	97.92	68.66	-0.03	0.41
2	99.78	76.08	100	76.90	0.21	1.07
3	97.21	83.67	97.65	82.39	0.45	-1.52
4	95.46	73.22	94.5	76.90	-1.00	5.024

TABLE III: Numerical SHRV values.

	HRV Indices					
Test	SDNN	COV	SDSD	RMSSD	NN50	pNN50
1	145.795	0.2526	127.612	208.473	89 %	80 %
2	148.204	0.25877	134.682	215.112	92 %	82 %
3	157.765	0.2627	145.81	228.87	89 %	83 %
4	158.5958	0.26372	139.015	221.3869	87 %	81 %

results is that our device provides one SpO_2 value and one heart rate value for one test (roughly 2 minute period of data collection). Conversely, values from the commercial device were averaged over that same period. Based on Table II, the values of SpO_2 and heart rate are consistent with the nominal adult range for SpO_2 and heart rate. Furthermore, the statistical figure R^2 is 0.9634 for SpO_2 and 0.8994 for the heart rate measurements.

TABLE IV: Expected HRV values from other works.

Ref	# of Partic-ipants	SDNN (ms)	COV	SDSD	RMSSD (ms)	NN50	pNN50 (%)
[9]	392	13-168	N/R	N/R	N/R	N/R	N/R
[7]	36	20-120	0.04-0.12	20-100	20-80	80-120	15-30

The third set of data collected is short-term heart rate variability, which includes six calculated parameters from the test series. The tabulated is documented in the following Table III. It can be seen from comparing our extracted values to the expected values in Table IV, that our measurements seem slightly skewed in the positive direction. Measurements for COV, SDSD, RMSSD, and pNN50 are all higher than their standard counterparts. This is most likely due to our peak detection algorithm. This conclusion is further supported by the fact that the pNN50 measurement is greater than the expected by roughly 50%, meaning that the proportion of NN intervals greater than 50 ms is approximately 80% rather than the expected 30%. All these measurements can be improved by improving the ADC input signal, optimizing our digital filtering, and testing more robust peak detection algorithms.

V. Conclusions

We have designed this prototype as a foundation for a flexible wearable sensor in pulse oximetry devices. To demonstrate the device's utility, we measured a patient's pulse oximetry and heart rate and compared it against a commercial device in the nominal patient levels. The results of the device show a maximum of 1% deviation from SPO_2 and a maximum of 5% of the heart rate between the Masimo device and the proposed MQP device. Additionally, more work could be

A) Masimo Pulse Oximeter Setup

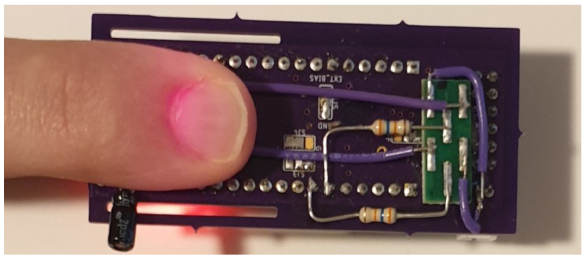
B) Proposed MQP Device

Fig. 2. Masimo Pulse Oximeter setup in A), MQP device setup in B)

done to evaluate the device's performance under deoxygenated states. Alongside additional improvements to the algorithms to extract major vitals. Ultimately, this demonstrates a successful implementation of a wearable sensor with hardware and algorithms to extract SpO_2, heart rate, short-term heart rate variability.

References

[1] B. Alberts, K. Hopkin, and D. Bray, "Essential cell biology," 2003.

[2] R. N. Pittman, *Oxygen Transport in Normal and Pathological Situations: Defects and Compensations*. Morgan and Claypool Life Sciences, 2011. [Online]. Available: https://www.ncbi.nlm.nih.gov/books/NBK54113/

[3] I. Costanzo, D. Sen, and U. Guler, "A prototype towards a transcutaneous oxygen sensing wearable," in *2019 IEEE Biomedical Circuits and Systems Conference (BioCAS)*, Oct 2019, pp. 1–4.

[4] D. Sen , I. Costanzo, and U. Guler, "Contemporary and Nascent Techniques for Monitoring of Oxygenation as a Vital Sign," in *IEEE International Midwest Symposium of Circuits and Systems, (MWSCAS)*, August 2020.

[5] D. N. Dutt and S. Shruthi, "Digital processing of ecg and ppg signals for study of arterial parameters for cardiovascular risk assessment," in *2015 International Conference on Communications and Signal Processing (ICCSP)*, 2015, pp. 1506–1510.

[6] P. Aroul, "Miniaturized pulse oximeter reference design," *Healthtech*, 2014. [Online]. Available: http://www.ti.com/lit/ug/tidu542/tidu542.pdf?ts=1588534192131

[7] W. Johnston, "Development of a signal processing library for extraction of spo2, hr, hrv, and rr from photoplethysmographic waveforms," *Masters Theses (All Theses, All Years)*, July 2006. [Online]. Available: https://digitalcommons.wpi.edu/etd-theses/919

[8] N. Sani, W. Mansor, Y. K. Lee, N. Zainudin, and S. A. Mahrim, "Determination of heart rate from photoplethysmogram using fast fourier transform," 05 2015, pp. 168–170.

[9] D. NUNAN, G. R. H. SANDERCOCK, and D. A. BRODIE, "A quantitative systematic review of normal values for short-term heart rate variability in healthy adults," *Pacing and Clinical Electrophysiology*, vol. 33, no. 11, pp. 1407–1417, 2010. [Online]. Available: https://onlinelibrary.wiley.com/doi/abs/10.1111/j.1540-8159.2010.02841.x